Observed changes in stratospheric circulation: Decreasing lifetime of N$_2$O, 2005-2021

Michael J. Prather[1], Lucien Froidevaux[2], Nathaniel J. Livesey[2]

[1]Earth System Science Department, University of California Irvine; Irvine, CA 92697-3100, USA
5 [2]Jet Propulsion Laboratory, California Institute of Technology; Pasadena, CA 91011, USA

Correspondence to: Michael Prather (mprather@uci.edu)

Abstract. Using Aura Microwave Limb Sounder satellite observations of stratospheric nitrous oxide (N$_2$O), ozone, and temperature from 2005 through 2021, we calculate the atmospheric lifetime of N$_2$O to be decreasing at a rate of -2.1±1.2 %/decade. This decrease is
10 occurring because the N$_2$O abundances in the middle tropical stratosphere, where N$_2$O is photochemically destroyed, are increasing at a faster rate than the bulk N$_2$O in the lower atmosphere. The cause appears to be a more vigorous stratospheric circulation, which models predict as a result of climate change. If the observed trends in lifetime and implied emissions continue, then the change in N$_2$O over the 21st Century will be 27% less than those
15 projected with a fixed lifetime, and the impact on global warming and ozone depletion will be proportionately lessened. Because global warming is caused in part by N$_2$O, this finding is an example of a negative climate-chemistry feedback.

1 Introduction

20

Projections of climate change include the acceleration of the stratospheric overturning circulation over the 21st century (Abalos et al., 2021). This three-dimensional circulation, condensed into a two-dimensional framework called the Brewer-Dobson Circulation (BDC), brings tropospheric air into the tropical stratosphere where it ascends, being photochemically
25 processed with ultraviolet radiation that increases with altitude, mixes across latitudes, and then descends at mid- to high-latitudes, re-entering the troposphere around mid-latitudes (Plumb and Mahlman, 1987; Neu and Plumb, 1999; Butchart, 2014). Observational metrics for an enhanced BDC are based on trends in the Age-of-Air (AoA) using surrogate gases such as SF$_6$. While models predict an enhanced BDC, the SF$_6$ observations indicate an
30 unchanged or decreasing BDC, but with large uncertainty (Karpechko et al., 2018; Abalos et al., 2021; Garney et al., 2022). The comparison of models and measurements of AoA has proven difficult (Fritsch et al., 2020). The search for BDC change with AoA has missed a more obvious and compelling case based on the important greenhouse gas nitrous oxide

(N$_2$O), where recent work has shown agreement in upper stratospheric trends across satellite
instruments and a model (Froidevaux et al., 2022). Here we take the Aura MLS observations
of N$_2$O, ozone (O$_3$), and temperature (T) from 2005 through 2021 and show that N$_2$O
increases through the middle tropical stratosphere, relatively greater than the rate of
tropospheric increases, lead to a shorter atmospheric lifetime, an important consequence of a
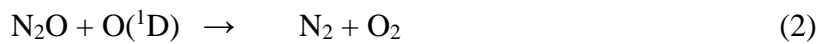more vigorous BDC.

Consequences of an enhanced BDC have recently focussed on the increased flux of
stratospheric ozone (O$_3$) into the troposphere with subsequent increase in tropospheric O$_3$, see
discussion in (Karpechko et al., 2018; Garney et al., 2022). Enhanced BDC also leads to
shorter lifetimes for gases like nitrous oxide (N$_2$O) and chlorofluorocarbons (CFCs) as
greater abundances are pushed higher in the tropical stratosphere where they experience
greater photolytic destruction. Two decades ago this mechanism was proposed by Butchart
and Scaife (2000) for the CFCs based on dynamical diagnostics of the BDC from a climate
model. Now we have observed and quantified this effect for a major greenhouse gas. Using
the simultaneous MLS vertical profiles of N$_2$O, O$_3$, and temperature, we calculate the total
loss of N$_2$O in the column, needing only the solar spectrum and absorption cross sections, as
in Prather et al. (2015, hence P2015). We find that the stratospheric N$_2$O loss rate is
increasing faster than the observed trend in surface N$_2$O, and hence the N$_2$O lifetime is
declining. For N$_2$O, a major greenhouse gas, it means that the climate impact of its
anthropogenic emissions will be reduced over this century; and for CFCs where we expect
parallel results, it means that these now-banned ozone-depleting gases will be cleaned out of
the atmosphere faster as shown by Butchart and Scaife (2001).
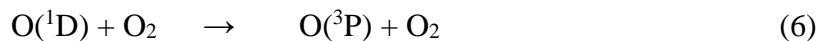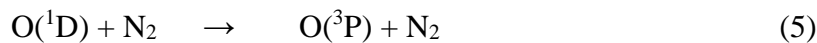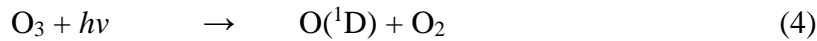
2 Measurements and methods

The Aura MLS observations of N$_2$O, O$_3$, and T are taken from the Goddard Earth Sciences
Data and Information Services Center in the form of Version 5 Level 3 monthly binned
profiles from August 2004 through December 2021 (Lambert et al., 2021; Schwartz et al.,
2021a, 2021b).   All data are averaged over the 72 longitude bins. There are 43 latitude
profiles every 4° (84°S to 84°N). Pressure levels range from 100 to 0.001 hPa with
logarithmic spacing, and the resolution depends on the MLS quantity. The very few negative
O$_3$ values (0.04% of data at 0.01 hPa) occur at the minimum in the O$_3$ profile and are
replaced with the mean value of 0.2 ppm, with negligible impact on photolysis rates. The

negative N_2O values are slightly more frequent (about 0.1% of data at 32 and 22 hPa, but 1.6% at 0.5 hPa where the mean value is 2.3 ppb). We do not wish to inflate the N_2O loss by

70 replacing negative values with large positive ones, so we opt for the safest choice and just replace negative N_2O values with 1 ppb, again, with negligible impact on N_2O loss. The N_2O vertical grid between 146 and 1 hPa (6 evenly spaced log(pressure) levels per decade) is coarser than that of O_3 and T (both use 12 intervals per decade). The missing N_2O levels in the O_3-T grid are calculated as the square-root of the product of the values on the adjacent

75 levels. For pressures <0.4 hPa, where MLS V5 N_2O data are not reported, we set the abundance to 0 ppb. Our consolidated MLS dataset then covers: 43 latitudes (84°S to 84°N), 37 pressure levels (100 – 0.001 hPa), and 209 months (Aug 2004 to Dec 2021).

The observational data consists of 8,987 independent column atmospheres. The top level

80 (0.001 hPa) is high enough that only a single layer of thickness 0.001 hPa with the same properties as the top layer is added to complete the atmosphere for the radiative calculation. Below 100 hPa, we add 6 layers with typical tropospheric values (320 ppt), however, these layers have negligible impact on N_2O loss because very little of the critical ultraviolet radiation reaches below 100 hPa. Each latitude profile is weighted by the area of the Earth

85 ±2 ° latitude on either side except for latitudes 1 (90 °S-82 °S) and 43 (82 °N-90 °N). For each column we calculate the profile of N_2O loss from photolysis (J-N_2O) and reaction with the electronically excited atomic oxygen $O(^1D)$ from the three reactions:

$$N_2O + h\nu \quad \rightarrow \quad N_2 + O \quad\quad\quad\quad (1)$$
$$N_2O + O(^1D) \quad \rightarrow \quad N_2 + O_2 \quad\quad\quad\quad (2)$$
$$N_2O + O(^1D) \quad \rightarrow \quad NO + NO \quad\quad\quad\quad (3)$$

The $O(^1D)$ is calculated from the O_3-T profiles assuming production equals loss

$$O_3 + h\nu \quad \rightarrow \quad O(^1D) + O_2 \quad\quad\quad\quad (4)$$
$$O(^1D) + N_2 \quad \rightarrow \quad O(^3P) + N_2 \quad\quad\quad\quad (5)$$
$$O(^1D) + O_2 \quad \rightarrow \quad O(^3P) + O_2 \quad\quad\quad\quad (6)$$

The radiative transfer calculation is the same as in Prather et al. (2015) and includes the solar

100 declination for the middle of each month, the sun-earth distance, but not the solar cycle (a mean solar flux is used).

Vertically, losses are weighted linearly in pressure (mass); and across latitude, they are weighted by the area of each latitude belt. Annually integrated budgets include the number of

105 days in each month, but leap-years are treated as 365-day years, and thus our annual losses are biased low by 0.07%. Lifetimes are budgetary time scales and calculated as a 12-month burden (TgN) divided by the 12-month loss (TgN/yr). The burden is calculated from monthly-mean, globally-averaged NOAA marine surface measurements (Dlugokencky, 2022) and using the conversion factor of 4.78 TgN/ppb (Prather et al., 2012). Given that the

110 gridding and source files have changed since P2015 (which used the 5° latitude GOZCARDS data), we compared the global monthly loss rates for the overlap period with P2015 (Aug 2004 – Dec 2011): the mean difference of 0.2% and rms difference of 0.6% show that both calculations are essentially identical. Uncertainty in the absolute N_2O lifetime is estimated at ±8 % (1-sigma), based primarily on the absolute calibration of MLS N_2O and the chemical

115 kinetics uncertainty, see Section 4 of P2015.

Uncertainties in trends here are calculated from a linear regression of the 12-month running averages of the monthly means as reported or calculated here. We select the 68% (1-sigma) range, because we are looking for 'likely' connections (68% confidence) rather than

120 'extremely likely' (95%). For example, the linear regression trend in N_2O loss uses the running averages and has 198 monthly points. The uncertainty is scaled up assuming there are only 17 yearly data points. As a check we recalculate the regression fit with the unsmoothed monthly data and get the same uncertainty.

125 **3 Results**

The primary calculation here is the annual N_2O loss (TgN/yr) shown in Figure 1a. It was surprising in that such a clear 17-year increase is apparent. Most of the interannual variability in this 12-month running mean time series is associated with the quasi-biennial

130 oscillation (see Ruiz et al., 2021). The linear regression gives a trend of +5.0±0.7 %/decade. This is larger than the +2.9±0.02 %/decade trend in the burden (Figure 1b), and results in an N_2O budgetary lifetime trend of -2.1±0.7 %/decade (Figure 1c). Our best estimate for the N_2O lifetime over the past decade (117 yr) is still close to that in P2015, which included other model calculations. Most important for the N_2O budget is the average loss itself, namely

135 13.43 TgN/yr with an interannual standard deviation of 3% and min-to-max range of 7%.

The primary source of stratospheric odd-nitrogen species (e.g., NO, NO_2, HNO_3) is production of NO in reaction (3), and we calculate the production of NO (Figure 1d), which (like the N_2O loss) also shows a positive trend of $+3.9\pm0.6$ %/decade.

140 The immediate cause of the lifetime trends (i.e., enhanced N_2O loss) can be an increase in the photochemical loss frequency or in the abundance of N_2O, or both. The critical zone for loss in the vertical is 3 to 30 hPa (80% of total loss), and in latitude it is 30°S to 30°N (75%), see P2015. Thus we focus on the tropical middle stratosphere. Photolysis (reaction 1) dominates loss here (by more than 90%) and the monthly mean J-N_2O at the equator (Figure 1e) shows
145 only a consistent decline across the critical region from -0.5 ± 0.1 %/decade at the top of the region (3 hPa) to -1.3 ± 0.3 %/decade at altitudes below 10 hPa. This change by itself would reduce the loss.

The declining J-N_2O is primarily due to the recovery of overhead ozone during this period
150 from reduced chlorine-catalysed depletion as the CFCs and other chlorinated gases have declined following the Montreal Protocol agreement that regulated these source gases (Bernath et al., 2020; Froidevaux et al., 2022; and references therein). Observations show continued increases in upper tropical stratospheric ozone for 2000–2020 (Godin-Beekmann et al., 2022) from a range of satellite measurements, including the MLS O_3 used here that is
155 driving the change of J-N_2O. For the upper stratospheric tropics (1-10 hPa), the generally observed O_3 trend of order $+1.0$ to $+1.6$ %/decade is consistent with the vertical pattern and magnitude of the J-N_2O trend. Another source of declining J-N_2O is the reduction in photolysis cross sections from lower temperatures. We calculate that the relative change in J in this altitude region is $+0.4$ %/K, and combining with the observed temperature trend of
160 about -0.5 K/decade (Maycock et al., 2018), we estimate the trend in J from temperature dependent cross sections is -0.2 %/decade and thus a small contribution to the total. The overall trend in J of about -1 %/decade reduces the N_2O loss and makes the disagreement between the burden and loss trends even greater.

165 Given that N_2O loss is increasing faster than the global burden by $+2.1$ %/decade, we expect that the N_2O abundances in the critical zone are likewise increasing faster. Because of the reduction in photolysis rates, we expect the abundance to be increasing at about $+6$ %/decade. Can we see this in the MLS N_2O data? The monthly mean 30°S-30°N N_2O abundances are shown in Figure 1f. The trends are clear but vary over altitude. At the bottom of the critical

zone (32 hPa) the trend is negative, -3.4±0.5 %/decade and probably due to a residual negative drift of the V5 MLS data in the lower stratosphere after 2010 as shown in Figure 16 of Livesey et al. (2021). It is unlikely to be real because suppression of vertical transport of N_2O below 30 hPa can hardly lead to increases in N_2O above and, moreover, the ACE-FTS data show positive trends at these pressures following the analysis of Froidevaux et al. (2022). The trend increases rapidly reaching +5.5±1.2 %/decade in the central zone (10 hPa) and +12.0±2.3 %/decade near the top (4.6 hPa). These increases are used directly in our calculation and average to +6 %/decade needed to explain the trend in total N_2O loss.

Are these increases in N_2O real or an artefact of a known calibration drift in the MLS 190 GHz observations, affecting mainly water vapor and N_2O? The MLS Version 5 dataset benefits from an extensive effort to remove/reduce drifts and verify the MLS H_2O and N_2O against the overlapping ACE-FTS satellite measurements, which are not believed to be drifting (Livesey et al., 2021; Froidevaux et al., 2022). The key comparison is Figure 16 of Livesey et al. (2021). In the tropics (20°S-20°N) there could be a small positive drift in MLS V5 N_2O versus ACE-FTS N_2O for the period 2005-2010 in the range 3-30 hPa, but for the later period 2010-2019, there is no drift, or even a negative drift at 30 hPa and below. This change with altitude may explain the small or negative trend in N_2O below 15 hPa. It is possible that N_2O is increasing throughout the tropical stratosphere if the negative trend at 32 hPa is due to instrumental drift. Parallel analysis of the MLS V4 N_2O (not shown) shows a similar increase in the trend from small negative trends at 32 hPa to large positive ones at 3 hPa (not shown). At the upper end of our range (2.2-6.8 hPa), Froidevaux et al. (2022, their Figure 12) find similar trends in N_2O to ours (~13 %/decade) from MLS, ACE-FTS, and a model. Their analysis included a much wider latitude range (50°S-50°N), but because N_2O abundances fall off rapidly outside of the tropical ascent region (see Figure 3 of Prather et al., 2015), the tropics should dominate the mean value and its trend. Thus, any calibration drift that impacts the lifetime (i.e., occurring in the critical region 3 to 30 hPa and 30°S to 30°N) is negligible compared to the increasing trend in N_2O loss (+5.0 %/decade). If the drift were slightly negative, correction would further increase this trend.

We believe that the solar cycle has had little impact on N_2O lifetime variability over the MLS Aura record here. The period 2005-2011 following Cycle 23 showed low activity (smoothed monthly sunspot number < 50); the peak of Cycle 24 (2011-2015) was among the lowest in the last 100 years; and Cycle 25 began in 2020 but activity remained low through 2021. We

conclude that the impact of the solar cycle on these observations was much less than the min-
to-max decrease in N_2O lifetime of 4-7 % (see P2015) and probably less than 2-3%.
Moreover, the symmetry of this low solar activity over 2005-2021 is unlikely to affect trends.

4 Implications

The recent WMO Ozone Assessments (Karpechko et al., 2018; Garny et al., 2022) concluded
that disagreement remains regarding the direction of the BDC trend between the chemistry-
climate model simulations (increasing rates) and the satellite observations of AoA tracers
(decreasing or uncertain). We present clear observational evidence supporting the models of
what is likely a climate-change driven increase in the net BDC using a major trace gas. N_2O
abundances in the tropical upper stratosphere are increasing at rates much faster than
tropospheric abundances, but this pattern cannot distinguish between more rapid ascent or
reduced mixing with extra-tropical latitudes. The latter would imply a slower growth rate for
extra-tropical N_2O, but this is not seen. If we perform a similar trend analysis to that shown
in Figure 1f for the extra-tropics (i.e., 30°N-58°N and 30°S-58°S), then we find an almost
identical pattern to that in the tropics: increasing at 7-8 %/decade versus 6 at 10 hPa; and at
14-18 %/decade versus 13 at 3.2 hPa, see Supplement Figure S1 and Table S6. The obvious
explanation is an increase in the meridional mean ascent rate in the tropics with little or no
change in mixing across the barrier between tropics and extra-tropics. The use of an
integrated quantity like the N_2O lifetime provides robust averaging over the large seasonal
and interannual variability of this gas in the middle and upper stratosphere. We expect these
results to hold for other gases with mid-stratosphere photolytic sinks, such as CFC-12.

Viewing the changing BDC in terms of lifetimes gives a different perspective of the potential
consequences of climate change. If this rate of change continues over the 21st century, then
the lifetimes of N_2O and CFC-12 might drop by 20%. Thus CFCs will be cleared out of the
atmosphere earlier than currently projected (e.g., Butchart and Scaife, 2001). The climate
impact of N_2O emissions will drop because their decay time will fall from 110 yr to 90 yr.
Note that the decay time of a pulse based on a lifetime of 117 yr is reduced by a factor of 0.94
due to chemical feedbacks (Prather, 1998; Prather et al., 2015). For example, if we
extrapolate the observed growth in N_2O burden over the last two decades (+2.9 %/decade),
we reach 419 ppb by 2100, a value between RCP6.0 and RCP8.5. If we use a constant

lifetime of 120 y to derive annual emissions and then re-project future N_2O using a declining lifetime (-2.1 %/decade), this value drops to 391 ppb. Over the 21st Century, the N_2O increase drops 27% from 103 ppb to 75 ppb, corresponding to a drop in effective radiative forcing of 0.09 W m^{-2}, equivalent to about 6.6 ppm CO_2 (Forster et al., 2021). Such differences are substantial when trying to tune our mitigation strategies to achieve climate change goals.

Overall, we will see an accelerated removal of the long-lived trace gases. Chipperfield et al. (2014) analyzed the change in CFC and N_2O atmospheric lifetimes with climate change (year 2100 versus 2000). For the five chemistry-climate models that calculated the N_2O lifetime, results were ambiguous: 2 increased, 1 decreased, and 2 were unchanged, all with absolute changes less than 0.5 %/decade. These results are not necessarily inconsistent with the projections here because the modeled scenarios included other chemical changes in the stratosphere and adopted a middling climate scenario (RCP 4.5). Chipperfield et al. also found that AoA metrics were a poor predictor of N_2O lifetime (see their Fig. 8-9). Thus, chemistry-climate model intercomparison projects should encourage the calculation of N_2O and CFC lifetimes over the 21st century as a major diagnostic of changing BDC, although accompanying changes in O_3 and T must also be diagnosed to evaluate the photochemically driven changes in lifetime.

There is an additional oddity in this analysis. We find that the production of NO (+3.9 %/decade) is increasing faster than the burden (+2.9 %/decade) but not as fast as N_2O loss (+5.0 %/decade), although the uncertainties overlap. This is expected because NO production peaks lower in the stratosphere and the rapid increase in loss above 10 hPa (~32 km) produces proportionally much less NO (see P2015, Figure 1). Reduced NO production relative to N_2O loss was also a theme in Nevison et al. (1999), who suggested that such changes might occur and be detectable in the observed ratio of NOy (NO and its products) to N_2O in the lowermost stratosphere. Our results are consistent with the analysis of Froidevaux et al. (2022), where the abundance of NO and NO_2 in the upper stratosphere is increasing at a rate much less than that of N_2O (approximately 2 vs. 12 %/decade). The abundance of NO in the tropical upper stratosphere, however, is a balance between production, vertical transport, and photochemical loss above 40 km, and we cannot estimate it from the production alone.

In parallel with our MLS N_2O data analysis, S.E. Strahan led a full chemistry-transport modeling study of the MLS period using the MERRA-2 wind fields and focusing on the chemistry of N_2O, NOy, and O_3. Their results support our analysis and show that more rapid vertical ascent in the tropical upper stratosphere is the cause of enhanced N_2O and N_2O loss.

275 This enhanced transport of NO led to its accumulation in the Arctic upper stratosphere with enhanced O_3 loss there. The modeled changes were shown to be driven by circulation changes, and they were matched by available satellite observations. That paper has now appeared (Strahan et al., 2022).

280 From the results here and in P2015, we assemble a budget for N_2O from pre-industrial to the last two decades (Table S7). Assuming that the pre-industrial stratospheric loss (10.5 TgN/y) is natural and has remained constant, then the anthropogenic emissions for the 2000s decade is 6.0 TgN/y and that for the 2010s decade is 7.6 TgN/y. This 27 %/decade increase in anthropogenic emissions comes primarily from the increasing N_2O atmospheric burden with

285 4 %/decade of the total coming from the decrease in N_2O lifetime derived here. Such growth in emissions shows how hard it will be to control them (Davidson, 2012) and identifies N_2O as a looming threat to climate stabilization.

Data Availability. The raw data used here were downloaded from the sites and at the dates

290 specified. The time series calculated here and shown in the figures are included in Tables S1-S5 & S8 in the Supplement.

Supplement. The Supplement related to this article is available online at: https://doi.org/10.5194/acp-22-.....

295

Author Contributions. MJP designed the research and performed the data analysis. LF and NJL analysed the accuracy of the datasets. MJP wrote the paper. LF and NJL reviewed and edited the paper.

300 *Competing interests*. The contact author has declared that neither they nor their co-authors have any competing interests

References

315 Abalos, M., Calvo, N., Benito-Barca, S., Garny, H., Hardiman, S. C., Lin, P., Andrews, M. B., Butchart, N., Garcia, R., Orbe, C., Saint-Martin, D., Watanabe, S., and Yoshida, K.: The Brewer–Dobson circulation in CMIP6, Atmos. Chem. Phys., 21, 13571–13591, https://doi.org/10.5194/acp-21-13571-2021, 2021.

Bernath P. F., Steffen J., Crouse J., and Boone C. D.: Sixteen-year trends in atmospheric trace 320 gases from orbit, J. Quant. Spectrosc. Ra. 253, 107178, https://doi.org/10.1016/j.jqsrt.2020.107178, 2020.

Butchart, N. (2014), The Brewer-Dobson circulation, Rev. Geophys.,52, 157–184, doi:10.1002/2013RG000448.

Butchart, N., Scaife, A.: Removal of chlorofluorocarbons by increased mass exchange 325 between the stratosphere and troposphere in a changing climate. Nature 410, 799–802, https://doi.org/10.1038/35071047, 2001.

Chipperfield, M.P., Q. Liang, S.E. Strahan, O. Morgenstern, S.S. Dhomse, N.L. Abraham, A.T. Archibald, S. Bekki, P. Braesicke, G. Di Genova, E.L. Fleming, S.C. Hardiman, D. Iachetti, C.H. Jackman, D.E. Kinnison, M. Marchand, G. Pitari, J.A. Pyle, E. Rozanov, 330 A. Stenke and F. Tummon, Multi-model estimates of atmospheric lifetimes of long-lived Ozone-Depleting Substances: Present and future, J. Geophys. Res., 119, 2555-2573, doi:10.1002/2013JD021097, 2014.

Davidson, E.A.: Representative concentration pathways and mitigation scenarios for nitrous oxide, Environ. Res. Lett. 7, 024005, doi:10.1088/1748-9326/7/2/024005, 2012.

335 Dlugokencky, E. (2022) Data from the NOAA web site, www.esrl.noaa.gov/gmd/ccgg/trends_n2o/ n2o_mm_gl.txt [pulled 2022-07-26], ed.dlugokencky@noaa.gov

Forster, P., T. Storelvmo, K. Armour, W. Collins, J.-L. Dufresne, D. Frame, D.J. Lunt, T. Mauritsen, M.D. Palmer, M. Watanabe, M. Wild, and H. Zhang, 2021: The Earth's 340 Energy Budget, Climate Feedbacks, and Climate Sensitivity. In Climate Change 2021: The Physical Science Basis. Contribution of Working Group I to the Sixth Assessment Report of the Intergovernmental Panel on Climate Change [Masson-Delmotte, V., P. Zhai, A. Pirani, et al., (eds.)]. Cambridge University Press, Cambridge, United Kingdom and New York, NY, USA, pp. 923–1054, doi:10.1017/9781009157896.009, 2021.

345 Fritsch, F., Garny, H., Engel, A., Bönisch, H., and Eichinger, R.: Sensitivity of age of air trends to the derivation method for non-linear increasing inert SF6, Atmos. Chem. Phys., 20, 8709–8725, https://doi.org/10.5194/acp-20-8709-2020, 2020.

Froidevaux, L., Kinnison, D. E., Wang, R., Anderson, J., and Fuller, R. A.: Evaluation of CESM1 (WACCM) free-running and specified dynamics atmospheric composition

350   simulations using global multispecies satellite data records, Atmos. Chem. Phys., 19, 4783–4821, https://doi.org/10.5194/acp-19-4783-2019, 2019.

Froidevaux, L., Kinnison, D. E., Santee, M. L., Millán, L. F., Livesey, N. J., Read, W. G., Bardeen, C. G., Orlando, J. J., and Fuller, R. A.: Upper stratospheric ClO and HOCl trends (2005–2020): Aura Microwave Limb Sounder and model results, Atmos. Chem.

355   Phys., 22, 4779–4799, https://doi.org/10.5194/acp-22-4779-2022, 2022.

Garny, H., H. Hendon (Lead Authors), M. Abalos, G. Chiodo, A. Purich, W. Randel K. Smith and D. Thompson, Scientific Assessment of Ozone Depletion: 2022, World Meteorological Organisation Global Ozone Research and Monitoring Project-Report No. XX, WMO/UNEP Scientific Assessment of Ozone Depletion: 2022. Chapter 5:

360   Stratospheric Ozone Changes and Climate, World Meteorological Organization, Geneva, Switzerland, 2022.

Godin-Beekmann, S., Azouz, N., Sofieva, V., Hubert, D., Petropavlovskikh, I., Effertz, P., Ancellet, G., Degenstein, D., Zawada, D., Froidevaux, L., Frith, S., Wild, J., Davis, S., Steinbrecht, W., Leblanc, T., Querel, R., Tourpali, K., Damadeo, R., Maillard-Barras, E.,

365   Stübi, R., Vigouroux, C., Arosio, C., Nedoluha, G., Boyd, I., and van Malderen, R.: Updated trends of the stratospheric ozone vertical distribution in the 60° S–60° N latitude range based on the LOTUS regression model, Atmos. Chem. Phys. Discuss. [preprint], https://doi.org/10.5194/acp-2022-137, accepted, 2022.

Karpechko, A., A. Maycock (Lead Authors), M. Abalos, J. Arblaster, H. Akiyoshi, C.

370   Garfinkel, K. Rosenlof and M. Sigmond, Scientific Assessment of Ozone Depletion: 2018, World Meteorological Organisation Global Ozone Research and Monitoring Project-Report No. 58, WMO/UNEP Scientific Assessment of Ozone Depletion: 2018. Chapter 5: Stratospheric Ozone Changes and Climate, World Meteorological Organization, Geneva, Switzerland, 2018.

375   Lambert, A., Livesey, N., Read, W., and Fuller, R., MLS/Aura Level 3 Monthly Binned Nitrous Oxide (N2O) Mixing Ratio on Assorted Grids V005, Greenbelt, MD, USA, Goddard Earth Sciences Data and Information Services Center (GES DISC), Accessed: [2022-05-06], 10.5067/Aura/MLS/DATA/3545, 2021.

Livesey, N. J., Read, W. G., Froidevaux, L., Lambert, A., Santee, M. L., Schwartz, M. J.,

380   Millán, L. F., Jarnot, R. F., Wagner, P. A., Hurst, D. F., Walker, K. A., Sheese, P. E., and Nedoluha, G. E.: Investigation and amelioration of long-term instrumental drifts in water vapor and nitrous oxide measurements from the Aura Microwave Limb Sounder (MLS) and their implications for studies of variability and trends, Atmos. Chem. Phys., 21, 15409–15430, https://doi.org/10.5194/acp-21-15409-2021, 2021.

385   Maycock, A. C., Randel, W. J., Steiner, A. K., Karpechko, A. Y., Christy, J., Saunders, R., et al.: Revisiting the mystery of recent stratospheric temperature trends. Geophysical Research Letters, 45, 9919–9933. https://doi.org/10.1029/2018GL078035, 2018.

Neu, J. L., and Plumb, R. A., Age of air in a "leaky pipe" model of stratospheric transport, J. Geophys. Res., 104(D16), 19243– 19255, doi:10.1029/1999JD900251, 1999.

390   Nevison, C.D., Keim, E.R., Solomon, S., Fahey, D.W., Elkins, J.W., Lowenstein, M., Podolske, J.R.: Constraints on N_2O sinks inferred from observed tracer correlations in the lower stratosphere, Global Biogeochemical Cycles, 13(3) 737-742, 1999.

Plumb, R. A., and J. D. Mahlman, The zonally-averaged transport characteristics of the GFDL general circulation/tracer model, J. Atmos. Sci.,44, 298–327, doi: 10.1175/1520-

395   0469(1987)044%3C0298:TZATCO%3E2.0.CO;2, 1987.

Prather, M.J., Time scales in atmospheric chemistry: coupled perturbations to N2O, NOy, and O3, Science, 279, 1339-1341, 1998.

Prather, M.J., C.D. Holmes, and J. Hsu, Reactive greenhouse gas scenarios: Systematic exploration of uncertainties and the role of atmospheric chemistry, Geophys. Res. Lett., 39, L09803, 5 pp., doi:10.1029/2012GL051440, 2012.

Prather, M.J., J. Hsu, N.M. DeLuca, C.H. Jackman, L.D. Oman, A.R. Douglass, E.L. Fleming, S.E. Strahan, and S.D. Steenrod, O.A. Søvde, I.S.A. Isaksen, L. Froidevaux, and B. Funke Measuring and modeling the lifetime of nitrous oxide including its variability, J. Geophys. Res. Atmos., 120, 5693–5705. doi: 10.1002/2015JD023267, 2015.

Ruiz, Daniel J., Michael J. Prather, Susan E. Strahan, Rona L. Thompson, Lucien Froidevaux, Stephen D. Steenrod, How atmospheric chemistry and transport drive surface variability of N2O and CFC-11. J. Geophys. Res.: Atmospheres, 126, e2020JD033979. https://doi.org/10.1029/2020JD033979, 2021.

Schwartz, M., Livesey, N., Read, W., and Fuller, R., MLS/Aura Level 3 Monthly Binned Temperature on Assorted Grids V005, Greenbelt, MD, USA, Goddard Earth Sciences Data and Information Services Center (GES DISC), Accessed: [2022-07-26] [Data Access Date], 10.5067/Aura/MLS/DATA/3550, 2021a.

Schwartz, M., Froidevaux, L., Livesey, N., Read, W., and Fuller, R., MLS/Aura Level 3 Monthly Binned Ozone (O3) Mixing Ratio on Assorted Grids V005, Greenbelt, MD, USA, Goddard Earth Sciences Data and Information Services Center (GES DISC), Accessed: [2022-05-06, yrs 2004 & 2021 re-pulled on 2022-07-06], 10.5067/Aura/MLS/DATA/3546, 2021b.

Strahan, S. E., Coy, L., Douglass, A. R., & Damon, M. R.: Faster tropical upper stratospheric upwelling drives changes in ozone chemistry. Geophys. Res, Letts., 49, e2022GL101075, https://doi.org/10.1029/2022GL101075, 2022
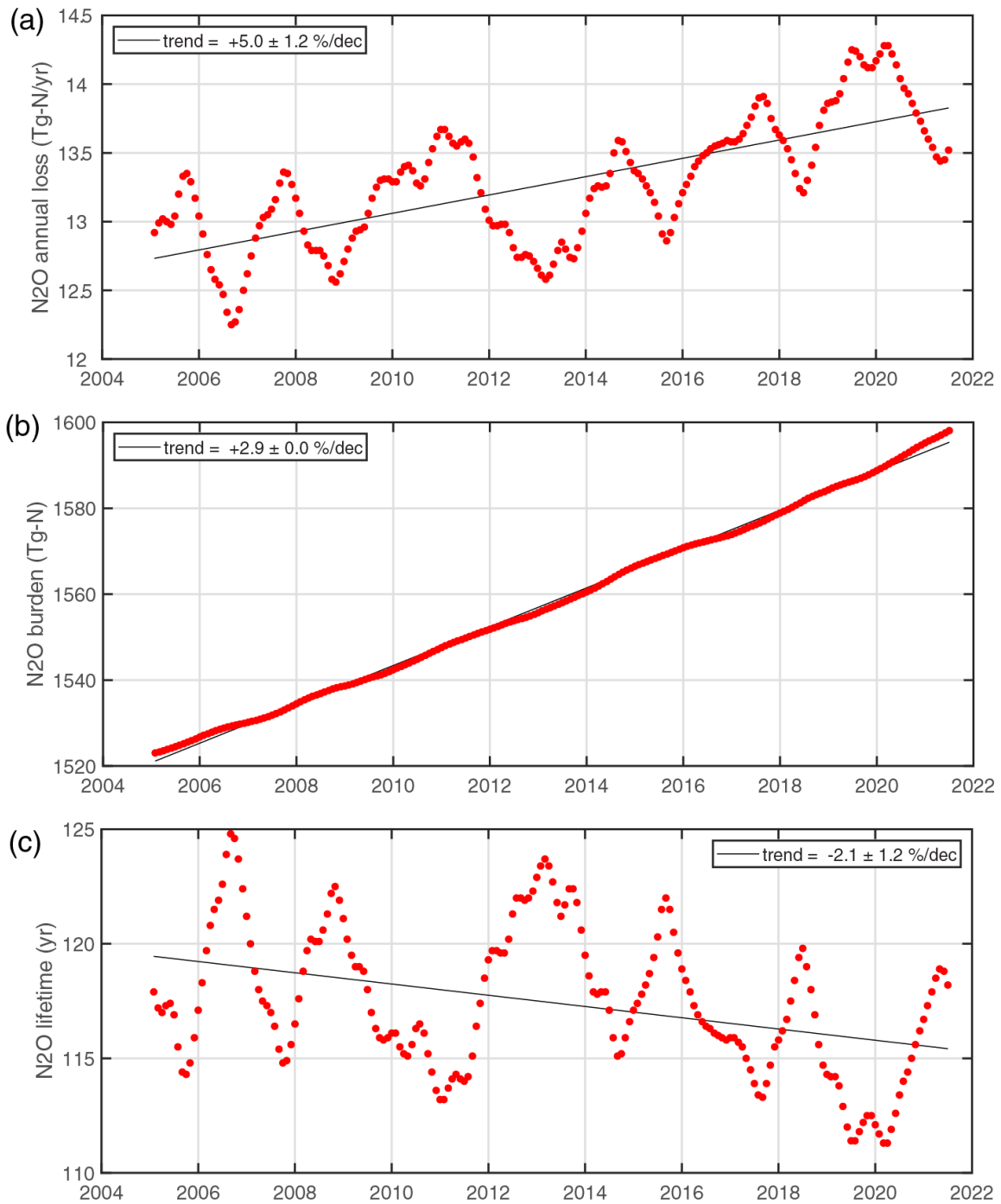
425

Figure 1abc. (a) N$_2$O loss rate (TgN/yr) as monthly values of a 12-month running mean. The 198 red points begin with the 12-month average of August 2004 through July 2005 plotted as February 1, 2005 with the final point being July 1, 2021 (all of 2021). The thin black trend line show the slope and uncertainty in the legend, see text. (b) N$_2$O global burden (TgN) based on marine surface observations. (c) N$_2$O lifetime derived from the

430   burden divided by loss rate. Production of NO (TgN/yr) from N$_2$O loss. (e) Stratospheric photolysis rates, j-N$_2$O (/s), at the standard MLS V5 T pressure levels (see legend) and averaged over 30°S-30°N. (f) N$_2$O abundance (ppb) at the standard V5 N$_2$O pressure levels (see legend) and averaged over 30°S-30°N.

435